Gene alterations in tumor-associated endothelial cells from endometrial cancer

XUE-LIAN DU[1,2], TAO JIANG[2], WEN-BO ZHAO[1], FEI WANG[1], GUI-LI WANG[1], MIN CUI[1] and ZE-QING WEN[1]

[1]Department of Obstetrics and Gynecology, Provincial Hospital affiliated to Shandong University, Jinan 250021; [2]Department of Gynecological Oncology, Shandong Tumor Hospital, Jinan 250117, P.R. China

Received June 13, 2008; Accepted August 11, 2008

DOI: 10.3892/ijmm_00000064

Abstract. The alterations in the gene expression profile of tumor-associated human endometrial endothelial cells (HEECs) may allow opportunities for developing new therapeutic approaches to inhibit angiogenesis in endometrial cancer. The aim of this study was to identify the different gene expression pattern between tumor-associated HEECs and normal HEECs. To elucidate the molecular mechanisms governing the abnormal vasculature in endometrial cancer, we examined global expression patterns of purified endothelial cells from three endometrial cancers and three age-matched normal endometria using oligonucleotide microarrays. We also performed *in vitro* culture and identified the endothelial origin, as well as observing the functional characteristics in angiogenesis, of HEECs from the two different sources. Microarray analyses revealed distinct gene expression patterns and consistent up-regulation of certain endometrial endothelial marker genes across patient samples. More than 300 genes that exhibited ≥2-fold differences were identified in tumor-associated HEECs. Pathway analysis showed that pathways of Cell cycle, Cell adhesion molecules (CAMs), focal adhesion, and extracellular matrix (ECM)-receptor interaction were obviously predominant. The results of the microarray analysis were confirmed by quantitative real-time PCR, immunohistochemistry, and/or Western blotting. Moreover, although the tumor-associated HEECs did not show faster proliferation than normal HEECs, they exhibited enhanced migration ability, potent invasiveness, and elevated tube formation *in vitro*. The present study shows that tumor and normal endothelium differ at the molecular level, and additional characterization of this gene expression database will provide insights into the angiogenesis of endometrial cancers and might be of great benefit for finding potential therapeutic targets.

Correspondence to: Dr Ze-Qing Wen, Department of Obstetrics and Gynecology, Provincial Hospital affiliated to Shandong University, Jinan 250021, P.R. China
E-mail: wzq23800@yahoo. cn

Key words: endometrial cancer, human endometrial endothelial cells, angiogenesis, microarray analyses

Introduction

Endometrial cancer is one of the most common malignancies of the female genital tract. Although early-stage endometrial cancer can be treated surgically, mortality in women with advanced disease has remained largely unchanged despite improvements in surgical technique, chemotherapy regimens, and radiation protocols (1-3). It is now well known that enhanced angiogenesis is relevant to an increased risk of metastasis and poor prognosis which makes it a very desirable therapeutic target in endometrial cancer (4-6).

Several studies indicated that tumor-associated vessels were structurally and functionally abnormal, with delayed maturation, increased permeability, and rapid proliferation (7,8). Tumor-specific endothelial genes and normal endothelial genes were define in a small number of breast, colon, brain and ovarian cancers using microarray analyses (9-12). However, the endometrium is a tissue unique for its cyclic destruction and rapid regeneration of blood vessels. The angiogenic behavior of endometrium endothelial cells is expected to differ from those in other tissues. To date, only a few reports have described the isolation and characterization of endothelial cells of the endometrium (13-15). The molecular characterization of these isolated human endometrial endothelial cells (HEECs) has been limited to the evaluation of estradiol and progesterone receptors, the vascular endothelial growth factor receptor type 2 (VEGFR-2), and several select endothelial markers. This lack of data prompted us to carry out expression profiling on purified endothelial cells from invasive endometrial cancers and normal endometrium. Profiling expression changes that occur in the vasculature of endometrial cancer provide insight into the mechanisms underlying tumor vascular growth and also reveal attractive targets for antiangiogenic therapies.

In the present study, we immunopurified endothelial cells from freshly resected specimens of three endometrial cancers and three normal endometrial tissues and investigated the gene expression profile using microarrays. The subset of genes identified in this study may represent candidate genes involved in the angiogenesis and development of endometrial

cancer. Moreover, we examined the growth characteristics and contrasted the capacity of immigration, invasiveness, and tube formation of isolated HEECs to find the different biological characteristics between tumor-specific and normal endothelium.

Materials and methods

Sample preparation. Fresh tissue samples of endometrial cancer were obtained from patients undergoing hysterectomies at the Shandong Tumor Hospital. The presence of endometrial cancer was confirmed by pathological diagnosis. Samples of normal endometrium were obtained from premenopausal women undergoing hysterectomy for benign gynecological diseases other than endometrial abnormalities. The patients selected for obtaining endometria had not been on hormonal medication for 6 months, and stages of the cycles were confirmed by histological examination and last menstruation period prior to the operations. Informed consent was obtained from all patients and the use of human specimens for these experiments was reviewed and approved by the committee of medical ethics, Shandong Tumor Hospital, Shandong province, P.R. China. The detailed information on case histories is listed in Table I. Since the endometrium is a tissue unique for its cyclic destruction and rapid regeneration of blood vessels, we chose patients with at same stage of the menstrual cycle to compare in this study.

The isolation and culture of HEECs were performed according to a previously reported procedure with a little modification (11). Three samples of endometrial cancer and three samples of normal endometria were used to isolate HEECs. The minced tissue was digested with 0.5% collagenase I at 37˚C for 30 min followed by filtration through a metal mesh (70 μm) screen for removal of the undigested tissue. Dual selection methods were used to ensure that any observed gene expression changes were pure HEECs. A number of negative selections were carried out, including red blood cell lysis (NH_4Cl) and removal of monocytes, lymphocytes, and granulocytes using anti-CD14, anti-CD45, and anti-CD64 beads (DynaBeads, Dynal Biotech, Brown Deer, WI). Positive selection was performed repeatedly with mouse anti-human CD31 antibodies and goat anti-mouse IgG-coated Dynabeads as described. 5-10x10^6 positively isolated cells were used for RNA isolation after purity analysis by flow cytometry, and others were cultured in endothelium culture medium (Dulbecco's modified Eagle's medium supplemented with 20 mM HEPES, 100 U/ml penicillin, 100 μg/ml streptomycin, 20% fetal bovine serum, 100 μg/ml ECGS, 40 U/ml heparin and 40 U/ml insulin; Gibco BRL, Gaithersburg, MD) in a fibronectin-coated culture flask.

Flow cytometry. Before carrying out microarray analysis, we tested the purity of all samples with the endothelial cell markers CD31 and von Willebrand factor (vWF). Cells (10^5) were incubated in PBS/5% FBS with rabbit anti-human vWF monoclonal antibody or mouse anti-human CD31 at room temperature for 45 min (Santa Cruz Biotechnology, Inc., Santa Cruz, CA). After washing, the cells were incubated with FITC-labeled rat anti-rabbit or goat anti-mouse monoclonal antibody for 30 min and suspended in cold buffer. Flow cytometry was conducted on a FACScalibur (Becton Dickinson Labware, Franklin Lakes, NJ).

Immunofluorescence staining. Cells were plated on coverslips and fixed with cold 4% paraformaldehyde for 15 min, permeabilized with 0.1% Triton X-100, then incubated with mouse anti-human CD31, CD34 or rabbit anti-human vWF for 1 h at room temperature. After washing, a fluorochrome-labeled secondary antibody (1:100) was added for 1 h. 4', 6-Diamidino-2-phenylindole was counterstained in some experiments, and the slides were mounted with antifade mounting medium (Santa Cruz Biotechnology, Inc.)

RNA isolation and oligonucleotide microarray analysis. Total RNA was harvested from endothelial cells using TRIzol (Invitrogen, Carlsbad, CA) and purified using the RNeasy Mini Kit and RNase-free DNase Set (Qiagen, Valencia, CA) according to the manufacturer's protocols. The quantity and quality of the purified RNA were assessed by OD260 and OD280 measurements on a spectrophotometer and the integrity was determined by formaldehyde denatured gel electrophoresis. The cDNA were synthesized by reverse transcription, purified, labeled with Cy3-dCTP and Cy5-dCTP, and hybridized to Affymetrix Human Genome U133 Plus 2.0 Array containing 47 000 transcripts according to the manufacturer's recommendations. The GeneChip arrays were washed and then stained (streptavidin-phycoerythrin) on an Affymetrix Fluidics Station 450 followed by scanning on a GeneChip Scanner 3000 and GeneChip Operating Software (Affymetrix, Santa Clara, CA). Array normalization and gene expression estimates were obtained using Affymetrix Microarray Suite 5.0 software (MAS5). Differential expression was determined using the combined basis of t-test with $P \leq 0.05$ and fold changes of 2-fold.

Quantitative real-time polymerase chain reaction (PCR) validation. To evaluate the reliability of microarray results, ten genes were randomly selected for further confirmation by real-time PCR. Total RNA (1 μg) was reverse transcribed in a total volume of 20 μl, and real-time PCR using SYBR green fluorescence was performed. Real-time quantitative polymerase chain reaction was performed on an ABI Prism 7000 Sequence Detection System using a SYBR Green RT-PCR Kit (Applied Biosystems, Foster City, CA). The primers used for real-time PCR were listed in Table II. The protocol of real-time PCR was as follows: initiation with a 10 min denaturation at 95˚C, followed by 40 cycles of amplification at 95˚C (10 sec) for denaturation, 55˚C (10 sec) for annealing and 72˚C for extension. All samples were run in triplicate. The real-time PCR amplification product was analyzed by melting curve analysis and 3% agarose gel electrophoresis, respectively. To calculate the relative expression for each gene, the $2^{-\Delta\Delta CT}$ method was used, averaging the CT values for GAPDH for a single reference gene value (16).

Immunohistochemical staining. Five of the ten genes were randomly selected to be confirmed by immunohistochemistry, others were testified using Western blotting. Paraffin sections were antigen-retrieved, blocked in normal horse serum, and

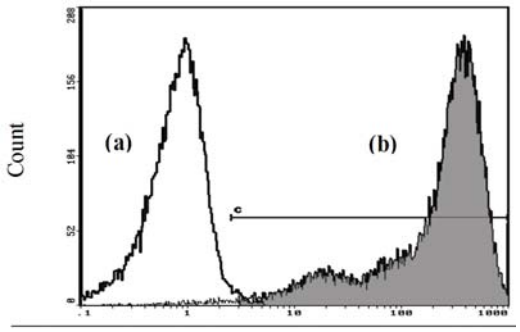

ID	%	Count	MnX	MdX	Min	Max
C	98.0	29394	195.0	300.6	2.61	1024

Figure 1. Detection of endothelial cell purity by flow cytometry. (a) Negative control; (b) HEECs purity in one sample of endometrial cancer. The immunopurification technique yielded endothelial cell purity of 98% in one sample of endometrial cancer.

incubated in the following antibodies: rabbit anti-endothelial cell-specific molecule 1(ESM1) at 1:100, rabbit anti-secreted phosphoprotein 1(SPP1) at 1:200 (BD Biosciences, Franklin Lakes, NJ), mouse anti-matrix metalloproteinase 10 (MMP10) at 1:50, anti-high-mobility group box 1 (HMGB1) at 1:200, or anti-Capping protein, gelsolin-like (CAPG) at 1:100 (Santa Cruz Biotechnology, Inc.) overnight at 4˚C. After three washes in PBS, sections were incubated with secondary antibody for 1 h at 37˚C. Positive reactions were detected by incubating the slides with stable 3,3-diaminobenzidine for 3-10 min. Sections were counterstained with Gill's hematoxylin for 30 to 60 sec. The intensity of protein expression in the endothelial cells was evaluated using Optimas 6.5 software.

Western blot analysis. Confluent cells were harvested and lysed with cold RIPA buffer. Total cell lysates were clarified by centrifugation (14,000 rpm, 20 min) at 4˚C. Total protein concentration was determined by BCA Protein Assay kit (Pierce, Rockford, IL). Then 20 μg of each soluble protein sample was separated by 10% or 15% SDS-polyacrylamide gel electrophoresis (PAGE) and transferred to a nitrocellulose membrane. After blocking with 5% TBST-milk (20 mmol/l Tris-HCl, 137 mM NaCl, 1.5% nonfat dry milk, and 0.1% Tween-20, pH 7.6), membranes were incubated with anti-LAMB1 (1:1000), anti-VIM (1: 500), anti-MMP9 (1:500) (Santa Cruz Biotechnology), anti-ABCC3 (1:2500), anti-CDC25B (1:1000), and anti-ß-actin (1:5000) (BD Biosciences, Franklin Lakes, NJ) antibodies overnight at 4˚C, respectively. Then the membranes were washed and incubated with horseradish peroxidase-labeled anti-rabbit or anti-mouse IgG antibody, respectively (Santa Cruz Biotech). After washing, the Western blot was developed using an enhanced chemiluminescence kit (Pierce, Rockford, IL). Detection was performed using the Dura West detection system (Pierce). Results were representative of four experiments.

Cell proliferation detection by MTT assay. HEECs in primary culture were detached by trypsin-EDTA and seeded in a 96-well plate (10^4 cells/well) in three parallel wells each at 37˚C in a 5% CO_2 humidified atmosphere. For non-cell control group, equal volume of medium was added. Cells were cultured for 24, 48, 72 and 96 h respectively, and viability was assessed using 20 μl 3-(4, 5-dimethylthiazol-2-yl)-2, 5-diphenyl tetrazolium bromide (MTT) (15 mg/ml, Sigma, St. Louis, USA) and incubated for a further 3 h. The medium was removed and 150 μl DMSO was added to each well. Optical density was read on a microplate reader at 570 nm using the DMSO as blank.

Wound healing assays of the endothelial monolayer. Confluent monolayers of endothelial cells were wounded using a micropipette tip (1 ml), rinsed with growth medium. Wound closure was monitored for 16 h and photographed using a digital camera. For quantitative presentation of the data, the percentage of the repaired area was quantified by computerized analysis of the digitized images.

Cell invasion assay. Endothelial cell migration was investigated using a modified Transwell chamber system. HEECs ($2x10^5$) were seeded on Matrigel-coated membrane inserts with a pore size of 8 μm (BD Bioscience, Heidelberg, Germany) in the presence of DMEM supplemented with 0.1% BSA. The lower chamber contained DMEM supplemented with 10% FCS, L-glutamine (10 mmol/l), basic fibroblast growth factor (0.5 ng/ml), epidermal growth factor (0.05 ng/ml) and endothelial cell growth-stimulating factor from bovine brain (ECGS/H, 0.2%). After 20 h at 37˚C in a humidified atmosphere with 5% CO_2, the cells on the upper side were scraped off with a rubber policeman and cells that had migrated into the lower compartment were fixed (4% paraformaldehyde in PBS), stained with H&E and counted from five random high power fields at x400 magnification in each well.

Tube formation assay. Matrigel (12.5 mg/ml; Becton Dickinson, San Jose, CA) was thawed at 4˚C and 50 μl were quickly added to each well of a 96-well plate. Matrigel-containing plates were allowed to incubate at 37˚C for 30 min and then seeded with endothelial cells at a density of $2x10^4$ cells/well. The wells were then incubated for 14 h at 37˚C. All of the experiments were carried out at least in triplicate.

Statistical analysis. The data are presented as mean ± SD. Data were analyzed with SPSS 10.0 statistical software (SPSS, Chicago, IL). The statistical differences between means were evaluated using the Student's t-test. Differences between two groups were determined using a P-value. A value of $P \leq 0.05$ was regarded as being statistically significant.

Results

Endothelial isolation and confirmation of cell purity. All samples were subjected to negative and positive immuno-selection and $1\text{-}5x10^7$ positively isolated cells were obtained from every sample. Flow cytometry revealed that the immunopurification technique yielded endothelial cell purity of ≥95% in all samples (Fig. 1 shows the HEEC purity in one sample of endometrial cancer).

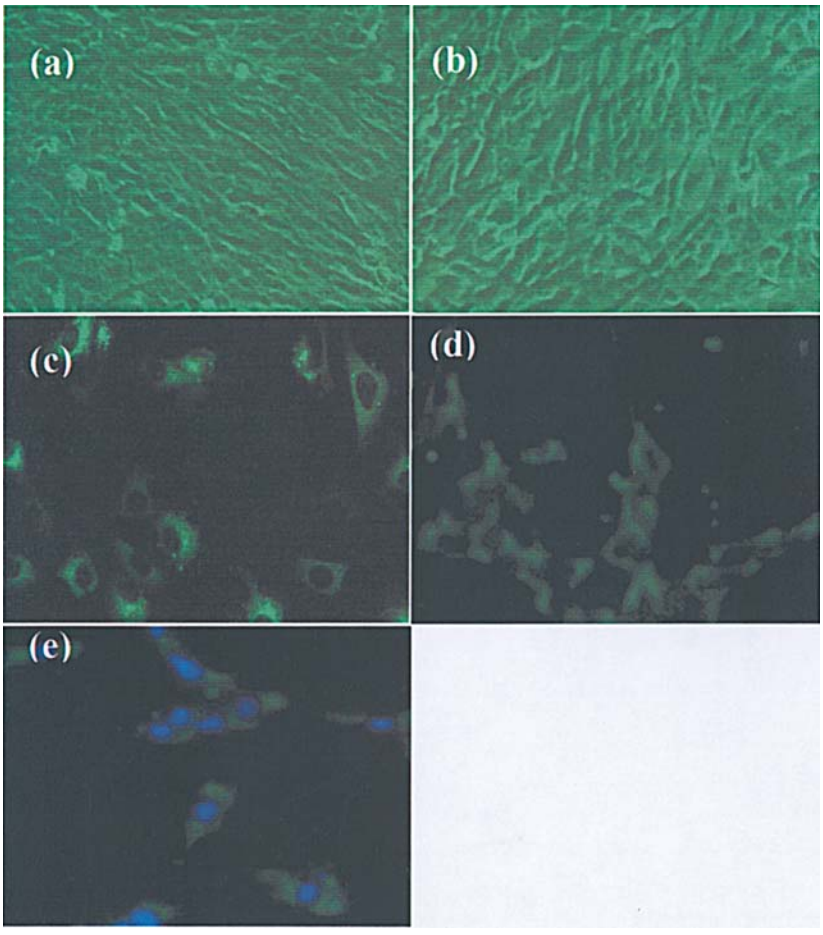

Figure 2. Morphology and characterization of purified endothelial cells. (a) Phase contrast photomicrograph of HEECs from normal endometria; (b) phase contrast photomicrograph of HEECs isolated from endometrial cancer. (c-e) Immunofluorescent staining: (c) vWF antigen; (d) CD31 antigen; (e) CD34 antigen. Original magnification. x200 (a and b), x400 (c-e).

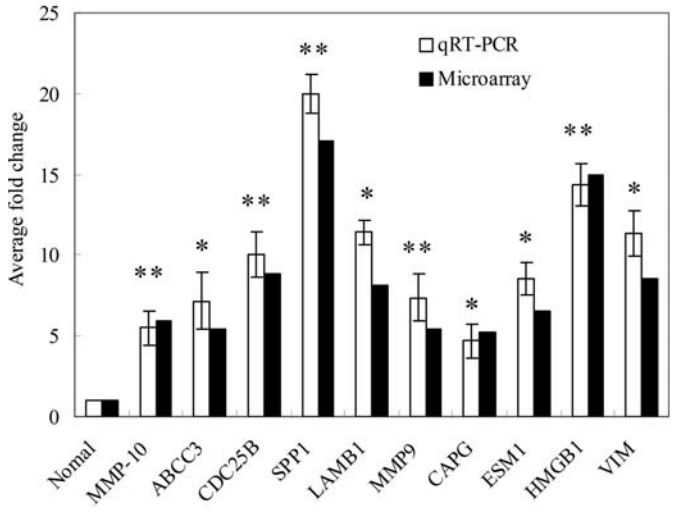

Figure 3. Quantitative real-time PCR validation of endothelial cell microarray data. Gene expression in 10 tumor isolates was calculated as a mean fold change relative to five normal endothelial specimens (normal, 1) using the 2-CT method. Real-time validation confirmed significant differential expression of 9 up-regulated genes, including MMP-10, ABCC3, CDC25B, SPP1, LAMB1, MMP9, CAPG, ESM1, HMGB1 and VIM, in tumor endothelial cells vs. normal isolates. $^{*}P\leq0.05$ vs. control; $^{**}P\leq0.01$ vs. control.

Characterization of isolated endothelial cells. HEECs separated from normal and malignant endometrial tissue presented similar appearance in culture medium under phase contrast microscope. Cell cultures presented flattened monolayers, with typical cobblestone morphology and contact-inhibition (Fig. 2A and B). All purified cells were characterized as endothelial cells on the basis of expression of the classical endothelial markers vWF, CD31, and CD34 as shown by immunofluorescence examination (Fig. 2C-E). In addition, the cells were negative when stained with antibodies recognizing the epithelial cell markers (keratin 8 and 6A), hematopoietic cells (CD14 and CD45), and smooth muscle cell actin (data not shown).

Genes up-regulated in endometrial tumor-associated HEECs. Total RNA from purified endothelial cells was subjected to microarray analysis using the Affymetrix Human U133 Plus 2.0 GeneChip platform. A multivariate permutation t test ($P\leq0.001$) identified 317 genes that were differentially regulated ≥2-fold in tumor-associated HEECs when compared with HEECs isolated from normal endometrium. There were 191 genes with ≥2-fold increase in expression in tumor endothelium. Table III represents genes that were expressed at least 5-fold higher in tumor-associated HEECs. Several proteins involved in the extracellular matrix function,

Table I. Case histories of subjects from whom endometria were used to isolate endothelial cells.

Paired cases	Age (years)	Indications for hysterectomy	Stage of the cycle	Microarray	qRT-PCR
C1	48	Endothelial cancer stage IA	Proliferative	+	+
N1	44	Myoma of uterus	Proliferative	+	+
C2	52	Endothelial cancer stage IIIA	Proliferative	+	+
N2	50	Serous cystadenoma	Proliferative	+	+
C3	54	Endothelial cancer stage IB	Secretory	+	+
N3	47	Benign cystic teratoma	Secretory	+	+

C, endometrial cancer; N, normal.

Table II. Sequences of primers used for qRT-PCR.

Gene symbol	Gene bank ID	Primer sequence	Annealing temperature (˚C)
MMP-10	NM_002425	F 5'- CCTGATGTTGGTGGCTTCAGT -3' R 5'- CTGGTGTATAATTCACAATCCTGTAGGT -3'	60
CDC25B	S78187	F 5'-TCTCATCTGAGCGTGGGC-3' P 5'-CTTCAGGCCTCGAAAGGC-3'	57
SPP1	NM_000582	F 5'- CTCCATTGACTCGAACGACTC -3 R 5'- CAGGTCTGCGAAACTTCTTAGAT -3	60'
LAMB1	NM_002291	F 5'-GGGTTCGTTAAGTTCCGTGT-3' R 5'-CACTCACAAGGTTTGCATCC-3'	58
ABCC3	NM_003786	F 5'-GCTCCAAGATCCTTTTAGCCAA-3' R 5'-GCCAAGATGAGGGCAGAGAGTA-3'	58
MMP9 '	NM_004994	F 5'-TGCCTGCAACGTGAACATCT-3 R 5'-CACTTGTCGGCGATAAGGAA-3'	60
ESM1	NM_007036	F 5'-CAGGCATGGATGGCATGAAG-3' R 5'-CTGACTGGCAGTTGCAGGTCTC-3'	57
HMGB1	NM_002128	F 5'-AATGGGCTGATAAAAGGTTTTG-3' R 5'-CTAACCCTGCTGTTCGCTTG-3'	59
VIM	NM_003380	F 5'-GTTTGGTCGCATATCGCAAC-3' R 5'-AATGCGCAGCACCAGGATAG-3'	60
CAPG	NM_001747	F 5'-CTCACAGCTGACAAGGCAAA-3 R 5'-CCACCCTCATTTCCAGTCC-3'	60
GAPDH	NM_002046	F 5'-GGGAGCCAAAAGGGTCATCATCTC-3' R 5'-CCATGCCAGTGAGCTTCCCGTTC-3'	57

F, forward primer; R, reverse primer.

such as SPP1, MMP9, LAMB1, MMP10, LOX, and LGALS3BP, had increased expression in tumor vasculature by changes of 17.1-, 5.4-, 8.2-, 5.9-, 5.9-, and 9.0-fold, respectively. Several proteins responsible for actin cytoskeleton organization and regulation, such as CAPG, CAPZA1 and TMSB10, were up-regulated by 5.1-, 8.2- and 5.6-fold, respectively. MAPRE1, CDC25B and CCNB2, genes correlating with regulation of the cell cycle, were also elevated in tumor endothelium.

Genes down-regulated in endometrial cancer endothelium. The reduction of gene expression in tumor versus normal vasculature may reveal a gene function to suppress tumor and/or vascular growth. We also identified genes that were down-regulated in endothelial cells derived from endometrial cancer tissue. There were 126 genes with ≥2-fold decrease in expression in tumor endothelium, with 25 decreased at least 5-fold (Table IV). Several genes with potential anti-angiogenic or antiproliferative roles, such as Cyclin-dependent

Table III. Genes up-regulated by 5-fold in the tumor-associated endothelium.

GeneBank ID	Name	Description	Fold	Chromosomal location	Function
L25081	RHOC	Ras homolog gene family, member C	7.452	1p13.1	Plays a role in I-κB kinase NF-κB cascade and small GTPase mediated signal transduction
NM_000129	F13A1	Coagulation factor XIII, A1 polypeptide	7.713	6p25.3-p24.3	Related to complement and coagulation
NM_000582	SPP1	Secreted phosphoprotein 1 (osteopontin, bone sialoprotein I early T-lymphocyte activation 1)	17.087	4q21-q25	Growth factor activity; cell-cell signaling skeletal development; regulation of cell proliferation; cell motility
NM_001546	ID4	Inhibitor of DNA binding 4, dominant negative helix-loop-helix protein	8.744	6p22-p21	Regulation of transcription from RNA polymerase II; transcription cofactor activity
NM_001549	IFIT4	Interferon-induced protein with tetratricopeptide repeats 4	7.014	10q24	Unknown
NM_001618	PARP1	Poly (ADP-ribose) polymerase family, member 1	5.553	1q41-q42	Fas pathway and stress induction of HSP regulation; response to DNA damage stimulus; DNA repair; transcription from RNA polymerase II promoter
NM_001747	CAPG	Capping protein (actin filament), gelsolin-like	5.177	2p11.2	Actin cytoskeleton organization and biogenesis; actin filament-based process
NM_001781	CD69	CD69 molecule	8.352	12p13-p12	Cell surface receptor linked signal transduction
NM_002128	HMGB1	High-mobility group box 1	5.008	13q12	Cell cycle; establishment and or maintenance of chromatin architecture
NM_002210	ITGAV	Integrin, α V (vitronectin receptor, α polypeptide, antigen CD51)	8.667	2q31-q32	Cell adhesion molecules (CAMs); regulation of actin cytoskeleton; focal adhesion; ECM-receptor interaction
NM_002291	LAMB1	Laminin, ß 1	8.178	7q22	Cell Communication; focal adhesion; ECM-receptor interaction
NM_002317	LOX	Lysyl oxidase	5.861	5q23.2	Lysyl oxidase
NM_002425	MMP10	Matrix metalloproteinase 10 (stromelysin 2)	5.881	11q22.3	Involved in the breakdown of extracellular matrix in embryonic development, reproduction, tissue remodeling, and disease processes
NM_003039	SLC2A5	Solute carrier family 2, member 5	8.026	1p36.2	Carbohydrate metabolism; plasma membrane
NM_003380	VIM	Vimentin	8.576	10p13	Cell communication; structural constituent of cytoskeleton;
NM_003404	YWHAB	Tyrosine 3-monooxygenase/ tryptophan 5-monooxygenase activation protein, ß polypeptide	6.652	20q13.1	Cell cycle; smooth muscle contraction; calcium regulation in cardiac cells;
NM_003457	ZNF207	Zinc finger protein 207	9.322	17q11.2	Unknown
NM_003786	ABCC3	ATP-binding cassette, sub-family C (CFTR/ MRP), member 3	5.449	17q22	ATPase activity, transmembrane movement of substances; nuclear receptors in ipid metabolism and toxicity
NM_003816	ADAM9	ADAM metallopeptidase domain 9 (meltrin γ)	14.611	8p11.23	Metalloendopeptidase activity; metallopeptidase activity;
NM_004390	CTSH	Cathepsin H	5.145	15q24-q25	Cysteine-type peptidase activity; lytic vacuole
NM_004994	MMP9	Matrix metallopeptidase 9 , (gelatinase B, 92 kDa gelatinase 92 kDa type IV collagenase)	5.437	20q11.2-13.1	Leukocyte transendothelial migration inhibition of Matrix Metalloproteinases; extracellular matrix
NM_005192	CDKN3	Cyclin-dependent kinase inhibitor 3 (CDK2-associated dual specificity phosphatase)	8.358	14q22	Regulation of cell cycle; regulation of cell proliferation; dephosphorylation
NM_005567	LGAL S3BP	Lectin, galactoside-binding, soluble, 3 binding protein	9.038	17q25	Extracellular space; extracellular matrix
NM_005596	NFIB	Nuclear factor I/B	8.020	9p24.1	DNA replication

Table III. (Continued)

GeneBank ID	Name	Description	Fold	Chromosomal location	Function
NM_006135	CAPZA1	Capping protein (actin filament) muscle Z-line, α 1	8.179	1p13.2	Actin cytoskeleton organization and biogenesis; cell motility
NM_006290	TNFAIP3	Tumor necrosis factor, α-induced protein 3	6.913	6q23	Regulation of metabolism; ubiquitin cycle; negative regulation of apoptosis
NM_006597	HSPA8	Heat shock 70kDa protein 8	11.084	11q24.1	Circadian exercise; protein folding; MAPK signaling pathway
NM_007022	CYB 561D2	Putative tumor suppressor	6.017	3p21.3	M phase of mitotic cell cycle; ubiquitin-dependent protein catabolism;
NM_007036	ESM1	Endothelial cell-specific molecule 1	6.496	5q11.2	Growth factor activity; cellular morphogenesis; regulation of growth
NM_012325	MAPRE1	Microtubule-associated protein, RP/EB family, member 1	6.048	20q11.1-11.23	Cell proliferation; regulation of cell cycle
NM_014937	INPP5F	Inositol polyphosphate-5- phosphatase F	6.489	10q26.11	Unknown
NM_015507	EGFL6	EGF-like-domain, multiple 6	11.079	Xp22	Regulation of cell cycle, proliferation, and developmental processes; extracellular space
NM_016076	C1orf121	Chromosome 1 open reading frame 121	5.213	1q44	Unknown
NM_016433	GLTP	Glycolipid transfer protein	6.365	12q24.11	Glycolipid transporter activity
NM_017443	POLE3	Polymerase (DNA directed), ε 3 (p17 subunit)	6.355	9q33	Nucleotidyltransferase activity; DNA replication
NM_017549	EPDR1	Ependymin related protein 1	6.369	7p14.1	A type II transmembrane protein similar to protocadherins cell adhesion molecules; calcium dependent cell adhesion
NM_020644	TMEM9B	TMEM9 domain family, member B	10.488	11p15.3	I-κB kinase NF-κB cascade;signal transducer activity
NM_021103	TMSB10	Thymosin, ß 10	5.592	2p11.2	Cytoskeleton; actin binding
NM_025130	HKDC1	Hexokinase domain containing 1	6.018	10q21.3	Energy derivation by oxidation of organic compounds; kinase activity
NM_030796	ECOP	EGFR-coamplified and overexpressed protein	8.054	7p11.2	Unknown
NM_030945	CTRP3	Complement-c1q tumor necrosis factor-related protein; likely ortholog of mouse CORS26	7.486	5p13-p12	Inorganic anion transport; anion transport
NM_032376	TMEM101	Transmembrane protein 101	5.850	17q21.31	I-κB kinase NF-κB cascade; signal transducer activity
NM_033380	COL4A5	Collagen, type IV, α 5	8.484	Xq22	Extracellular protein; encodes one of the six subunits of type IV collagen, the major structural component of basement membranes.
NM_138376	TTC5	Tetratricopeptide repeat domain 5	6.564	14q11.2	Known as Strap
NM_138455	CTHRC1	Collagen triple helix repeat containing 1	6.745	8q22.3	Inorganic anion transport
NM_138462	ZMYND19	Zinc finger, MYND-type containing 19	8.646	9q34.3	May associate with tubulin
NM_17886	CKLFSF8	Chemokine-like factor superfamily 8	6.335	3p22.3	Regulates EGF-induced signaling; regulates cell proliferation
NM_212539	PRKCD	Protein kinase C, δ	5.515	3p21.31	Fc ε RI signaling pathway; Tight junction; skeletal development ; enzyme inhibitor activity positive regulation of cell
NR_001562	ANXA2	Annexin A2	8.745	15q21-q22	Proliferation; regulation of cell
S78187	CDC25B	Cell division cycle 25B	8.788	20p13	cycle; cell division; MAPK signaling pathway

Table IV. Genes down-regulated by 5-fold in the tumor-associated endothelium.

GeneBank ID	Name	Description	Fold	Chromosomal location	Function
NM_000077	CDKN2A	Cyclin-dependent kinase inhibitor 2A	0.138	9p21	Negative regulation of cell proliferation; enzyme inhibitor activity; cell cycle
NM_000090	COL3A1	Collagen, type III, α 1	0.044	2q31	Inorganic anion transport; Inflammatory Response Pathway
NM_000765	CYP3A7	Cytochrome P450, family 3, subfamily A, polypeptide 7	0.072	7q21-q22.1	Microsome; response to chemical substance; oxidoreductase activity
NM_001349	DARS	Aspartyl-tRNA synthetase	0.147	2q21.3	protein complex assembly; translation; ligase activity; Alanine and aspartate metabolism
NM_001532	SLC29A2	Solute carrier family 29, member 2	0.159	11q13	Cell proliferation
NM_001904	CTNNB1	catenin (cadherin-associated protein), ß 1, 88 kDa	0.144	3p21	Cell to Cell Adhesion Signaling; WNT Signaling Pathway; regulation of transcription from RNA polymerase II promoter; leukocyte transendothelial migration
NM_002461	MVD	Mevalonate (diphospho) decarboxylase	0.124	16q24.3	Lipid biosynthesis; lyase activity; kinase activity; steroid metabolism;
NM_002573	PAFAH1B3	Platelet-activating factor acetylhydrolase, isoform Ib, γ subunit (29 kD)	0.052	19q13.1	Soluble fraction; carboxylic ester hydrolase activity
NM_002865	RAB2A	RAB2, member RAS oncogene family	0.156	8q12.1	Intracellular protein transport; small GTPase mediated signal transduction
NM_003017	SFRS3	Splicing factor, arginine/serine-rich 3	0.166	6p21	RNA splicing
NM_003587	DHX16	DEAD/H box polypeptide 16	0.184	6p21.3	mRNA processing; RNA splicing; helicase activity; regulation of cell cycle
NM_003620	PPM1D	Protein phosphatase 1D magnesium-dependent, δ isoform	0.054	17q23.2	Phosphoprotein phosphatase activity; dephosphorylation; negative regulation of cell proliferation; regulation of cell cycle
NM_004095	EIF4EBP1	Eukaryotic translation initiation factor 4E binding protein 1	0.124	8p12	Negative regulation of cellular metabolism; translation factors; insulin signaling
NM_005738	ARL4A	ADP-ribosylation factor-like 4	0.108	7p21-p15.3	GTPase activity; small GTPase mediated signal transduction
NM_006191	PA2G4	Proliferation-associated 2G4, 38 kD	0.188	12q13.2	Metallopeptidase activity; cell proliferation;
NM_006770	MARCO	Macrophage receptor with collagenous structure	0.041	2q12-q13	Inorganic anion transport
NM_006821	ACOT2	acyl-CoA thioesterase 2	0.157	14q24.3	Lipid metabolism; coenzyme metabolism; fatty acid metabolism
NM_015922	NSDHL	NAD(P) dependent steroid dehydrogenase-like; H105e3	0.107	Xq28	Lipid biosynthesis; cholesterol biosynthesis; steroid metabolism;
NM_019903	ADD3	Adducin 3 (γ)	0.104	10q24.2-q24.3	Structural constituent of cytoskeleton; calmodulin binding;
NM_020401	NUP107	Nuclear pore complex protein	0.197	12q15	Protein transport; nuclear transport; endomembrane system;
NM_024027	COLEC11	Collectin sub-family member 11	0.107	2p25.3	Inorganic anion transport; humoral immune response; carbohydrate binding
NM_032603	LOXL3	Lysyl oxidase-like 3	0.091	2p13	Formation of crosslinks in collagens and elastin; may play a role in developmental regulation, senescence, tumor suppression, cell growth control, and chemotaxis
NM_145183	PYCARD	Apoptosis-associated speck-like protein containing a CARD	0.098	16p12-p11.2	Enzyme activator activity; induction of apoptosis; positive regulation of apoptosis
NM_206917	NGFRAP1	Nerve growth factor receptor (TNFRSF16) associated protein 1	0.133	Xq22.2	Apoptosis
NM_207043	ENSA	Endosulfine α	0.099	1q21.2	Response to chemical substance

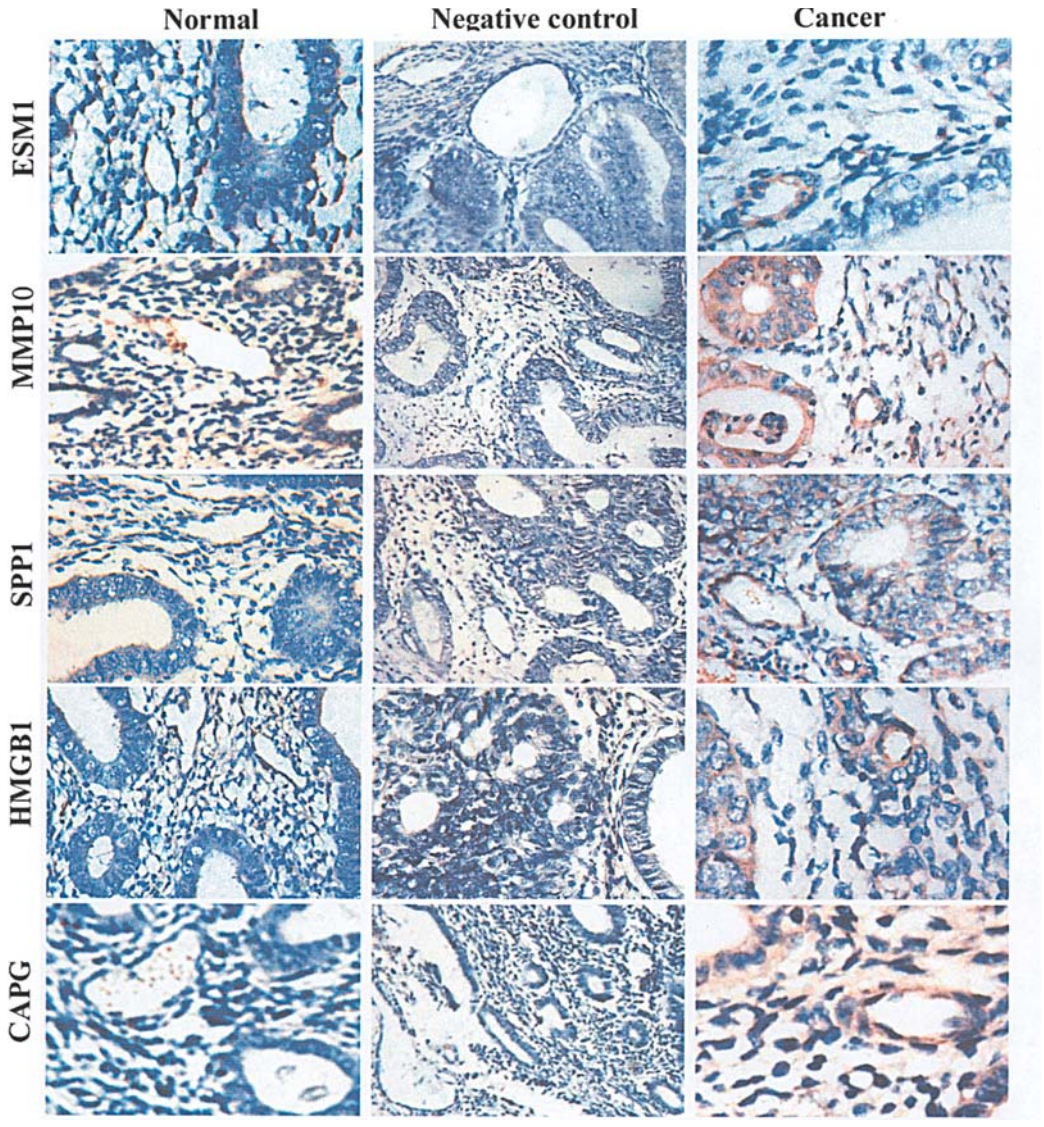

Figure 4. Immunohistochemical staining for ESM1, MMP10, SPP1, HMGB1, and CAPG in human normal endometria and endometrial cancers. All photomicrographs were taken at original magnification (x200 or x400).

kinase inhibitor 2A (CDKN2A) and Solute carrier family 29 member 2 (SLC29A2), were down-regulated by 7.2- and 6.3-fold, respectively. Nerve growth factor receptor associated protein 1 (NGFRAP1) and apoptosis-associated speck-like protein containing a CARD (PYCARD), genes responsible for the induction of apoptosis, were down-regulated by 7.5- and 9.2-fold, respectively. Catenin ß1(CTNNß1), an important factor of cell to cell adhesion signaling, was decreased by 6.9-fold.

Pathway analysis. All 317 differentially expressed genes were analyzed using Molecular Annotation System 2.0 (MAS 2.0, www.capitalbio.com) which integrates three pathway resources-KEGG, BioCarta and GenMAPP. The pathways are ranked with statistical significance by calculating their P-values based on hypergeometric distribution (17). Table V lists the significant pathways associated with cell survival. Among these, the pathways of cell cycle, cell adhesion molecules (CAMs), focal adhesion, and extracellular matrix (ECM)-receptor interaction have predominated.

Validation of gene expression alterations. To show the reproducibility of the microarray analysis, 10 genes were selected at random, spanning a range of fold-changes (5.2-29.1, Fig. 3). The microarray analysis identified MMP10 (13.8-fold), ABCC3 (5.4-fold), CDC25B (8.8-fold), SPP1 (29.1-fold), LAMB1 (8.2-fold), MMP9 (18.4-fold), CAPG (5.2-fold), ESM1 (6.5-fold), HMGB1 (15.0-fold), and VIM (8.6-fold) as being significantly increased in tumor-associated HEECs, and these changes were validated by real-time RT-PCR. Fig. 3 shows relative gene expression compared with normal HEECs. These data provide important confirmation of the gene expression alterations identified by the microarray analysis.

Immunohistochemical staining and Western blot analysis. Increased expression of ESM1, MMP10, SPP1, HMGB1, and CAPG was confirmed at the protein level by immuno-histochemical peroxidase staining in the tumor-associated vascular endothelia (Fig. 4) in all samples of endometrial cancer. A negative staining procedure (the same staining

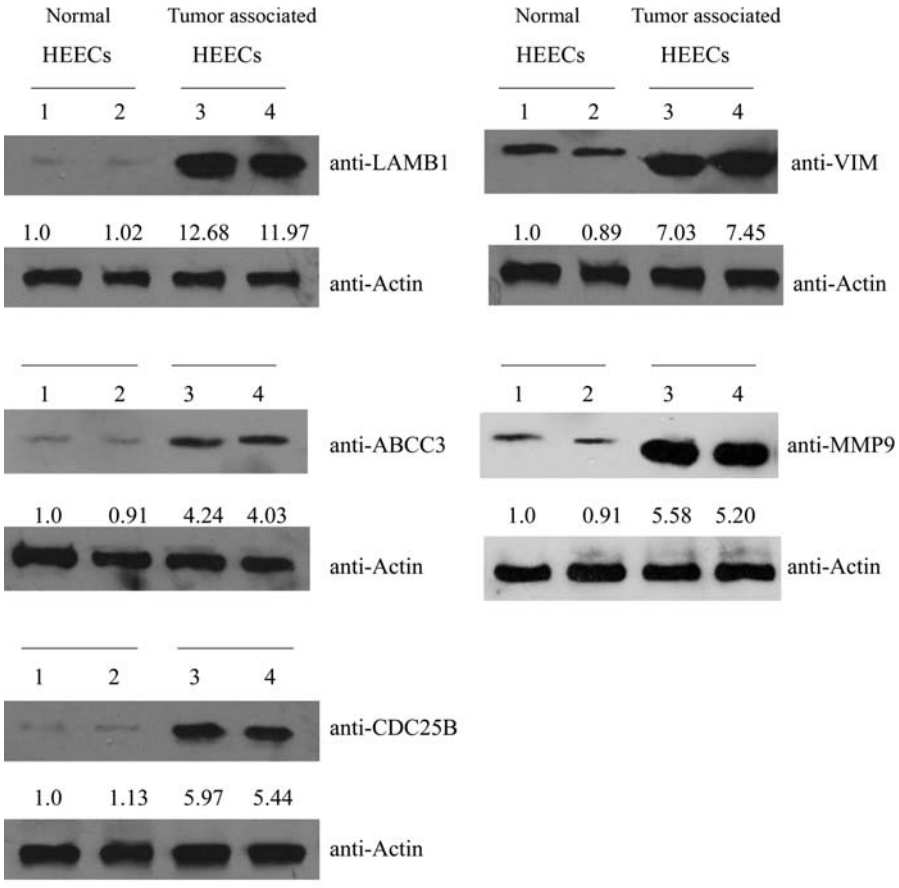

Figure 5. Western blot showing LAMB1, VIM, ABCC3, MMP9 and CDC25B protein in normal HEECs and tumor-associated HEECs. Representative experiments are shown.

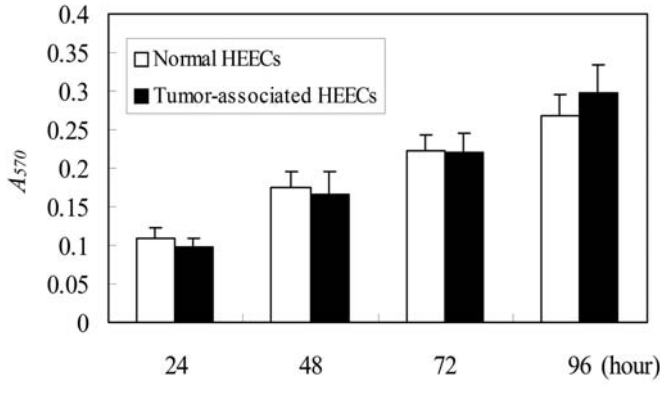

Figure 6. Proliferation assay of normal HEECs and tumor-associated HEECs. After cells were cultured for 24, 48, 72 and 96 h, there was no significant difference in proliferation rate of tumor-associated HEECs and normal HEECs.

procedure but without the primary antibody) showed no staining of the vessels. Western blot analysis showed higher LAMB1, VIM, MMP9, ABCC3, and CDC25B protein in tumor-associated HEECs (Fig. 5).

Proliferation of HEECs. As shown in Fig. 6, after cells were cultured for 24, 48, 72 and 96 h, there was no significant difference in the proliferation rate of tumor-associated HEECs and normal HEECs ($P \geq 0.05$). The results revealed that endothelial cells isolated from endometrial cancer do not proliferate faster than HEECs isolated from normal endothelium *in vitro*.

Wound healing assay of the endothelial monolayer. The wound healing assay is a widely-used procedure that allows an examination of cell migration in response to an artificial wound produced on a cell monolayer. Fig. 7 shows a significantly enhanced migration in tumor-associated HEECs compared with normal HEECs under the same conditions, with the percentage of repaired area of 16.37±2.88 vs. 37.54±5.63 ($P \leq 0.01$). These results indicate that tumor-associated HEECs presented an augmented effect on wound healing ability.

Cell invasion assay of HEECs. The invasion of endothelial cells is also one of the critical features in the formation of new blood vessels. To determine the endothelial cell invasion, we investigated the invasion ability of HECCs through Transwell inserts. Significantly more cells were detected in the lower chamber in tumor-associated HEECs than in the control group (131±22 vs. 189±31, $P \leq 0.05$, Fig. 8).

Tube formation assay of HEECs. The production of tubular structures is another important step in angiogenesis. HEECs plated on Matrigel aligned to form capillary-like structures

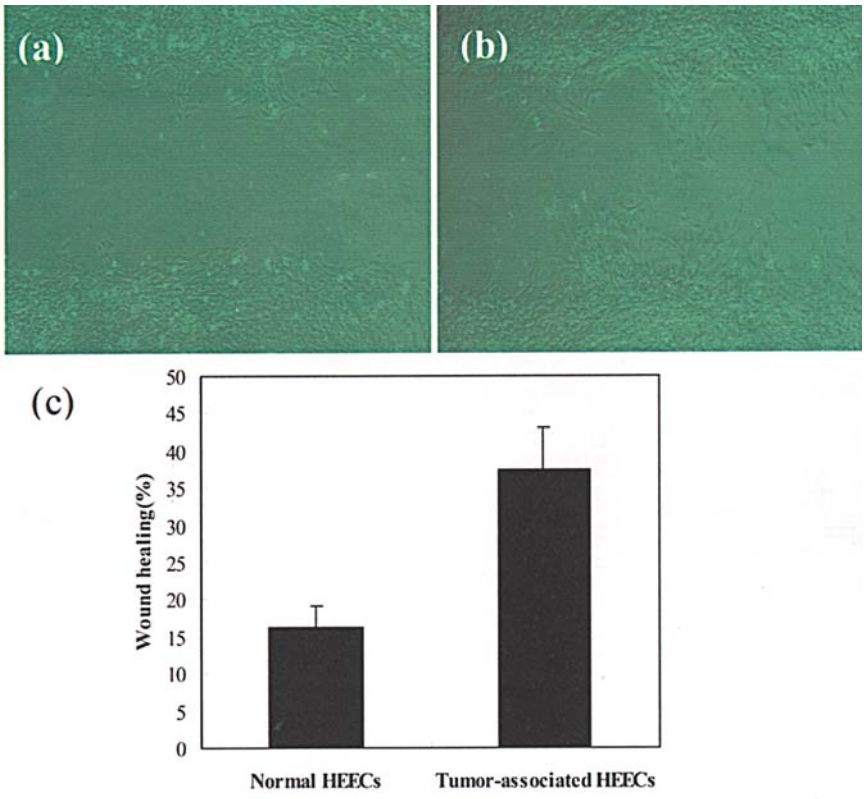

Figure 7. Wound healing assay of the endothelial monolayer. (a) Phase contrast photomicrographs of wounds in endothelial cell monolayers from normal endometrium; (b) wounds in endothelial cells from endometrial cancer. Original magnification, x100. (c) The percentage of repaired area of endothelial cells. $^{**}P \leq 0.01$ vs. control.

with multicentric junctions (Fig. 9). More tube-like structures were observed in tumor-associated HEECs than normal HEECs (56±18 vs. 31±16, $P \leq 0.05$). These data indicate that tumor-associated HEECs were functionally more powerful in angiogenesis than normal HEECs.

Discussion

It is well known that endothelial cells vary phenotypically depending on the organ of origin (14). There are limited data concerning genomic differences in tumor-associated endothelial cells from colon, breast, brain, and ovarian tumors (9-12). Previous global expression profile analysis has examined the normal endometria of normal cycling women and compared these data to different histological types of endometrial cancers (15). However, no data regarding tumor-associated endothelial cells from endometrial cancer have been evaluated using microarray analysis until now. To the best of our knowledge, this is the first study of genomic profiling of endometrial tumor-associated endothelial cells.

The endometrium is one of the most dynamic tissues in mammals due to the constantly changing levels of ovarian steroids which are believed to drastically affect gene expression. In order to minimize the change of gene expression caused by alteration in ovarian steroids, we chose to examine endothelial cells isolated from malignant and normal endometrial tissues matched for age and the period of menstrual cycle.

The major finding of the present study is that endometrial tumor-associated endothelial cells contain a large number of gene alterations in comparison with normal endometrial endothelial cells and, therefore, were likely to reflect differences in the ability of angiogenesis of endometrial cancer. Pathway analyses of these overexpressed genes showed that pathways of cell cycle, cell adhesion molecules (CAMs), focal adhesion, and extracellular matrix (ECM)-receptor interaction were obviously predominant. Loss of tumor suppressor activities was also found in our gene array analysis and several genes with potential antiangiogenic or antiproliferative roles were also depressed.

Data from our study shows that SPP1 and LAMB1, genes related to ECM (extracellular matrix) -receptor interaction, were obviously elevated in tumor-related endothelium. SPP1 (The cytokine/extracellular matrix protein osteopontin, OPN) is an integrin-binding protein overexpressed in various experimental models of malignancy and appears to be involved in tumorigenesis and metastasis in several types of cancers (18-20). Hirama and colleagues reported that culture medium with murine neuroblastoma C1300 cells transfected with SPP1 gene significantly stimulates human umbilical vein endothelial cell migration and induces neovascularization in mice by dorsal air sac assay (21). Moreover, Leali and colleagues found SPP1 expression was elevated in the newly formed endothelium of the chick embryo chorioallantoic membrane (CAM) and of murine s.c. Matrigel plug implants (22). Recombinant SPP1, the fusion protein GST-SPP1, and

Table V. Significant pathways involved in the specific phenotype of endothelial cells from endometrial cancer.

Pathway Name	Gene	Fold change	P-value	Q-value
MAPK signaling pathway	CDC25B	8.788		
	HSPA8	11.084	0.040498	0.0
	PRKCD	5.5152		
	CDC25B	8.788		
	CDKN2A	0.3118		
	YWHAB	6.6523		
Cell cycle	EGFL6	11.079	0.0	0.0
	PCNA	2.1749		
	COL3A1	0.2244		
	CTNNB1	0.2144		
	LAMB1	8.178		
Focal adhesion	SPP1	17.087		0.0
	BIRC3	2.1397	0.004141	
	COL3A1	0.2244		
	LAMB1	8.178		
ECM-receptor interaction	SPP1	17.087		0.0
	ITGB7	2.541	0.024879	
	CAPG	5.177		
Actin cytoskeleton organization	CAPZA1	8.179	0.006825	0.0
and biogenesis	FOS	0.3434		
Toll-like receptor signaling pathway	CD14	0.3921	0.138972	0.0
	CLDN4	2.1914		
	ITGB7	5.514		
	ITGAM	2.17174		
	ICAM1	0.4957		
Cell adhesion molecules (CAMs)	CLDN7	0.4279	5.0E-5	0.0
mTOR signaling pathway	EIF4EBP1	0.2248	0.083687	0.0
	CTNNB1	0.2144		
Wnt signaling pathway	CCND3	0.3991	0.238018	0.0
TGF-ß signaling pathway	ID4	8.7446	0.144675	0.0

FC, fold change; The q-value of a gene in SAM results is a false discovery rate for the gene list that includes the gene and all genes that are more significant.

the deletion mutant GST-DeltaRGD-SPP1 were angiogenic in the CAM assay. These results strongly implied that SPP1 had played an important role in tumor growth through the enhancement of angiogenesis *in vivo*. Previous studies indicated that SPP1 induced endothelial cell migration and up-regulated endothelial cell migration induced by VEGF (23,24). However, the effect of SPP1 on tumorigenesis as an angiogenic factor remains to be clarified. In the present work, we report the up-regulated expression of SPP1 in tumor-associated HEECs. The same conclusion had been drawn in the vasculature from ovarian cancers as well (12). Positive SPP1 expression with a consistent cytoplasmic localization in tumor-associated vasculature was observed in malignant human endometrium by immunohistochemistry or Western blotting. We therefore presume that SPP1 plays an important role in neovascularization of endometrial cancer, and further investigation should be conducted in the future.

The other up-regulated gene related to ECM -receptor interaction in the present study is LAMB1 (laminin, ß1 chain), which is a constituent of laminin-8. Laminins are major components of vascular and parenchymal basement membranes, which have been implicated in a wide variety of biological processes including cell adhesion, differentiation, migration, signaling and metastasis. LAMB1 is now known to be involved in cell adhesion, positive regulation of epithelial cell proliferation and cell migration. Experimental evidence described by Fujita and colleagues have identified three basement membrane laminins that share the same ß1 chain (LAMB1), namely laminin-2, laminin-8, and laminin-10, as new breast carcinoma angiogenic markers and may associate with breast tumor progression (25). A similar switch from ß2-containing to ß1-containing vascular laminins has also been shown to occur during the progression of brain gliomas and may constitute a general feature of vascular basement membrane changes in solid tumors (26). No data regarding the expression of this gene in endometrial cancer have been reported until now. The relationship between overexpressed LAMB1 in endothelial cells and angiogenesis in endometrial cancer is still unknown.

Matrix metalloproteinase (MMP)-mediated degradation of the extracellular matrix is a key point in tumor development and expansion. In the present study, we found elevated

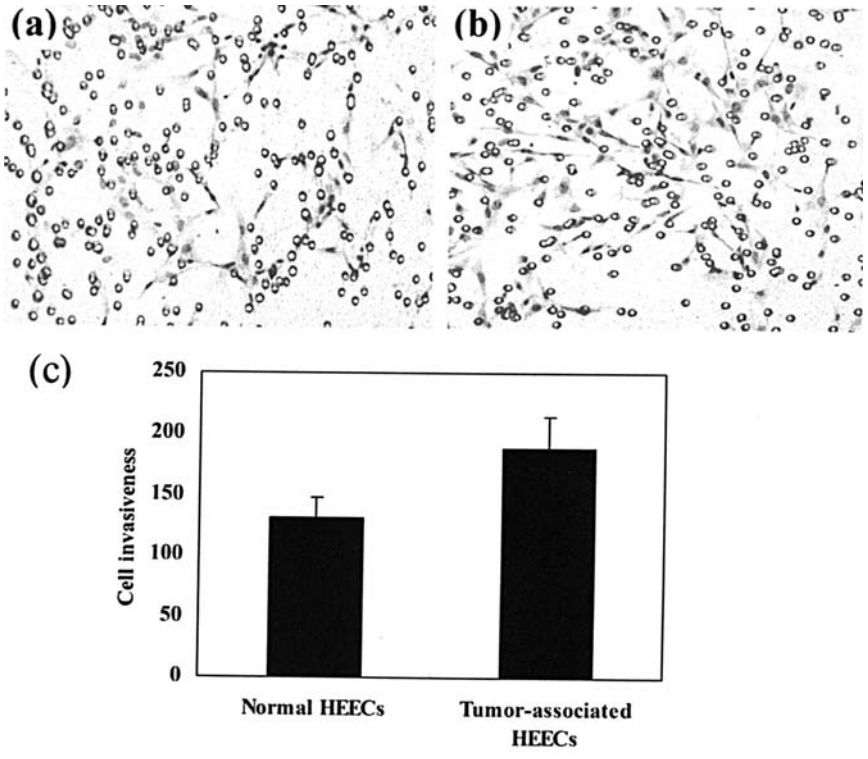

Figure 8. Relative invasion by endothelial cells from normal endometria and endometrial cancers. (a and b) Endothelial cells were on the lower surface of the transwell filters (magnification, x200). (a) Endothelial cells from normal endometrium; (b) endothelial cells from endometrial cancer. (c) The number of cells that invaded through the filters was counted under a microscope (magnification, x400) in five views. Columns, mean of three independent experiments; bars, SD. $^{*}P \leq 0.05$ vs. control.

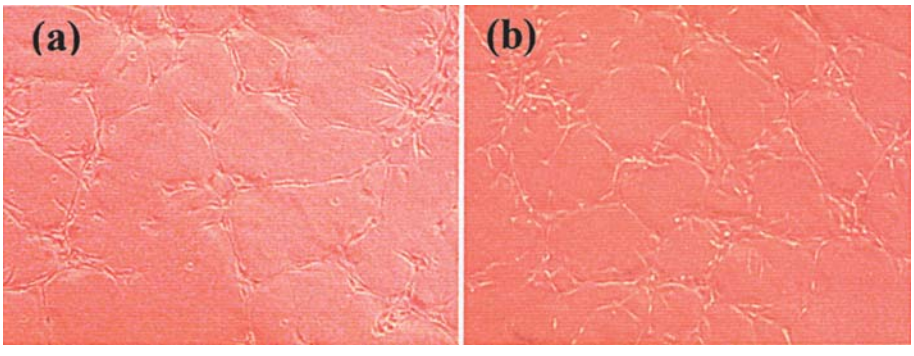

Figure 9. Tube formation of endothelial cells from normal endometrium and endometrial cancer. Cells cultured on Matrigel for 14 h, then photographed under a microscope (magnification, x200) and branching points were counted. (a) Endothelial cells from normal endometrium; (b) endothelial cells from endometrial cancer.

expression of MMP9 and MMP10 in endometrial tumor-related endothelium. MMP9 is one of the most important and well-characterized members of the MMP family and is considered to be closely associated with angiogenesis, which had been verified in breast and ovarian cancer (9,12). Karahan and colleagues found MMP-9 was expressed in a high percentage of endometrial carcinomas and their expression may be associated closely with vascular and lymphatic invasion (27). Moreover, MMP10 (stromelysin-2), previously not known to be related to angiogenesis, is now presumed to degrade various components of the extracellular matrix in disease processes, such as arthritis and metastasis. Several studies found increased expression of MMP10 in prostate and gastric cancers compared to benign tissues (28,29). Van Themsche and colleagues provided evidence that overexpression of MMP10 promoted lymphoid tumor development (30). MMP10 was dramatically overexpressed in metastatic non-small cell lung cancer compared with non-metastatic disease in a study examined by suppression subtractive hybridization and mircroarray (31). These results implied that there might be some relationship between MMP9 and MMP10 and the enhancement of angiogenesis in some malignant diseases. In our study, general immunohisto-chemial expression of MMP9 in stromal, epithelial and endothelial cells were detected in endometrial cancer. Increased expression of MMP9 and MMP10 in endometrial endothelia indicated that these two MMPs might be associated with promoted angiogenesis in malignant

endometrium although their precise mechanism still awaits investigation.

Degradation of the extracellular matrix, endothelial cell migration and the production of tubular structures are important steps in angiogenesis. The results of the present investigation show that tumor-associated HEECs migrated faster in wound healing assay than normal HEECs. Likewise, tumor-associated HEECs migrated through a Matrigel-coated filter faster and yielded more tube-like structures. These data indicated that tumor-associated HEECs were more functionally powerful in angiogenesis although they did not proliferate faster than normal HEECs *in vitro*. Some simultaneously activated signaling pathways, such as MAPK and TGF-ß signaling pathway, may play an important role in angiogenesis. At the same time, some depressed signaling pathways, such as mTOR and Wnt signaling pathway, may also participate in this process. However, their roles in endometrial tumor-associated angiogenesis and the signals that regulate their expression remain unknown.

In summary, the gene expression profiles derived in the current study define unique alterations in vascular gene expression in endometrial carcinoma. Our findings may be useful not only as an aid in characterizing the function of tumor-specific HEEC genes in endometrial cancer, but also as a means to find potential targets to achieve further gains in therapeutic benefit. Additional work is needed to define the role of the novel genes identified here in processes of endometrial cancer angiogenesis.

Acknowledgements

This work was supported by the grants from The Shandong Provincial Natural Science Foundation (No. Y2006C88).

References

1. Burke C, Foley M, Lenehan P, Kelehan P and Flannelly G: Early stage endometrial carcinoma-a study of management and outcome. Ir Med J 100: 621-623, 2007.
2. Zusterzeel PL, Bekkers RL, Hendriks JC, Neesham DN, Rome RM and Quinn MA: Prognostic factors for recurrence in patients with FIGO stage I and II, intermediate or high risk endometrial cancer. Acta Obstet Gynecol Scand 87: 240-246, 2008.
3. Ayhan A, Taskiran C, Celik C, Yuce K and Kucukali T: The influence of cytoreductive surgery on survival and morbidity in stage IVB endometrial cancer. Int J Gynecol Cancer 12: 448-453, 2002.
4. Sivridis E: Angiogenesis and endometrial cancer. Anticancer Res 21: 4383-4388, 2001.
5. Ozbudak IH, Karaveli S, Simsek T, Erdogan G and Pestereli E: Neoangiogenesis and expression of hypoxia-inducible factor 1alpha, vascular endothelial growth factor, and glucose transporter-1 in endometrioid type endometrium adenocarcinomas. Gynecol Oncol 108: 603-608, 2008.
6. Kamat AA, Merritt WM, Coffey D, *et al*: Clinical and biological significance of vascular endothelial growth factor in endometrial cancer. Clin Cancer Res 13: 7487-7495, 2007.
7. Morikawa S, Baluk P, Kaidoh T, *et al*: Abnormalities in pericytes on blood vessels and endothelial sprouts in tumors. Am J Pathol 160: 985-1000, 2002.
8. Baluk P, Morikawa S, Haskell A, Mancuso M and McDonald DM: Abnormalities of basement membrane on blood vessels and endothelial sprouts in tumors. Am J Pathol 163: 1801-1815, 2003.
9. Parker BS, Argani P, Cook BP, *et al*: Alterations in vascular gene expression in invasive breast carcinoma. Cancer Res 64: 7857-7866. Erratum in: Cancer Res 64: 8794, 2004.
10. St Croix B, Rago C, Velculescu V, *et al*: Genes expressed in human tumor endothelium. Science 289: 1197-1202, 2000.
11. Madden SL, Cook BP, Nacht M, *et al*: Vascular gene expression in nonneoplastic and malignant brain. Am J Pathol 165: 601-608, 2004.
12. Lu C, Bonome T, Li Y, Kamat AA, *et al*: Gene alterations identified by expression profiling in tumor-associated endothelial cells from invasive ovarian carcinoma. Cancer Res 67: 1757-1768, 2007.
13. Sha G, Wu D, Zhang L, *et al*: Differentially expressed genes in human endometrial endothelial cells derived from eutopic endometrium of patients with endometriosis compared with those from patients without endometriosis. Human Reprod 22: 3159-3169, 2007.
14. Langley RR, Ramirez KM, Tsan RZ, Van Arsdall M, Nilsson MB and Fidler IJ: Tissue-specific microvascular endothelial cell lines from H-2K(b)-tsA58 mice for studies of angiogenesis and metastasis. Cancer Res 63: 2971-2976, 2003.
15. Maxwell GL, Chandramouli GV, Dainty L, Litzi TJ, Berchuck A, Barrett JC and Risinger JI: Microarray analysis of endometrial carcinomas and mixed mullerian tumors reveals distinct gene expression profiles associated with different histologic types of uterine cancer. Clin Cancer Res 11: 4056-4066, 2005.
16. Livak KJ and Schmittgen TD: Analysis of relative gene expression data using real-time quantitative PCR and the $2^{(-\Delta\Delta C(T))}$ method. Methods 25: 402-408, 2001.
17. Mao X, Cai T, Olyarchuk JG and Wei L: Automated genome annotation and pathway identification using the KEGG Orthology (KO) as a controlled vocabulary. Bioinformatics 21: 3787-3793, 2005.
18. Agrawal D, Chen T, Irby R, *et al*: Osteopontin identified as lead marker of colon cancer progression, using pooled sample expression profiling. J Natl Cancer Inst 94: 513-521, 2002.
19. Briese J, Schulte HM, Bamberger CM, Löning T and Bamberger AM: Expression pattern of osteopontin in endometrial carcinoma: correlation with expression of the adhesion molecule CEACAM1. Int J Gynecol Pathol 25: 161-169, 2006.
20. Coppola D, Szabo M, Boulware D, Muraca P, Alsarraj M, Chambers AF and Yeatman TJ: Correlation of osteopontin protein expression and pathological stage across a wide variety of tumor histologies. Clin Cancer Res 10: 184-190, 2004.
21. Hirama M, Takahashi F, Takahashi K, *et al*: Osteopontin overproduced by tumor cells acts as a potent angiogenic factor contributing to tumor growth. Cancer Lett 198: 107-117, 2003.
22. Leali D, Dell'Era P, Stabile H, *et al*: Osteopontin (Eta-1) and fibroblast growth factor-2 cross-talk in angiogenesis. J Immunol 171: 1085-1093, 2003.
23. Shijubo N, Uede T, Kon S, Nagata M and Abe S: Vascular endothelial growth factor and osteopontin in tumor biology. Crit Rev Oncog 11: 135-146, 2000.
24. Takano S, Tsuboi K, Tomono Y, Mitsui Y and Nose T: Tissue factor, osteopontin, alphavbeta3 integrin expression in microvasculature of gliomas associated with vascular endothelial growth factor expression. Br J Cancer 82: 1967-1973, 2000.
25. Fujita M, Khazenzon NM, Bose S, *et al*: Overexpression of beta1-chain-containing laminins in capillary basement membranes of human breast cancer and its metastases. Breast Cancer Res 7: 166-167, 2005.
26. Ljubimova JY, Fujita M, Khazenzon NM, Ljubimov AV and Black KL: Changes in laminin isoforms associated with brain tumor invasion and angiogenesis. Front Biosci 11: 81-88, 2006.
27. Karahan N, Güney M, Baspinar S, Oral B, Kapucuoglu N and Mungan T: Expression of gelatinase (MMP-2 and MMP-9) and cyclooxygenase-2 (COX-2) in endometrial carcinoma. Eur J Gynaecol Oncol 28: 184-188, 2007.
28. Riddick AC, Shukla CJ, Pennington CJ, *et al*: Identification of degradome components associated with prostate cancer progression by expression analysis of human prostatic tissues. Br J Cancer 92: 2171-2180, 2005.
29. Aung PP, Oue N, Mitani Y, *et al*: Systematic search for gastric cancer-specific genes based on SAGE data: melanoma inhibitory activity and matrix metalloproteinase-10 are novel prognostic factors in patients with gastric cancer. Oncogene 25: 2546-2557, 2006.
30. Van Themsche C, Alain T, Kossakowska AE, Urbanski S, Potworowski EF and St-Pierre Y: Stromelysin-2 (matrix metalloproteinase 10) is inducible in lymphoma cells and accelerates the growth of lymphoid tumors in vivo. J Immunol 173: 3605-3611, 2004.
31. Lin TS, Chiou SH, Wang LS, *et al*: Expression spectra of matrix metalloproteinases in metastatic non-small cell lung cancer. Oncol Rep 12: 717-723, 2004.